Ghorbaninezhad and Ghorbaninezhad *Journal Of Nanostructure in Chemistry* 2013, **3**:53
http://www.jnanochem.com/content/3/1/53

Journal of Nanostructure in Chemistry
a SpringerOpen Journal

ORIGINAL Open Access

Simulation of nanodrug by theoretical approach

Saeideh Ghorbaninezhad* and Maryam Ghorbaninezhad

Abstract

In recent years, HIV-1 integrase (IN) has become an attractive target for designing antiretroviral agents. The development of raltegravir and other successful lead IN inhibitors has also influenced the IN inhibitor design strategy. This has led to the identification of several potent inhibitors in these last 2 years. The medicines which have the compound of C-centered and N-centered anti-HIV inhibitor with single-walled carbon nanotube are examined by density functional theory (DFT) method. In this paper, the end of the nanotubes, which was saturated with hydrogen atoms, was examined by DFT at the level of B3LYP and 6-31G(d) standard basis set. There are free Gibbs energy, free Helmholtz energy, enthalpy, bond length (Å), bond angle (in degrees), dihedral angle (in degrees), energy hyperconjugation, total energy (in Kcal mol^{-1}), moment dipole (in Debye), occupancy between nanotube (6, 6), and chalcone derivative. These cases and medicines show that complex 2 is more stable than the other complexes.

Keywords: NBO; Nanodrug; DFT; Chalcone; Inhibitor; Anti-HIV; Nanotube; SWCNT

Background

Since the discovery of carbon nanotubes by Iijima [1], extensive research has been devoted to their structural characterization [2]. Among the numerous delivery systems currently under investigations, carbon nanotubes (CNTs) seem to embody a promising option [3]. Pristine carbon nanotubes (pCNTs) are made up of carbon atoms arranged in a series of condensed benzene rings and wrapped into a tubular form (Figure 1). Concerning their use in biological systems, lack of solubility (both in organic solvents and aqueous solutions), formation of thick and inhomogeneous bundles, circulation half-life of 3 to 3.5 h [4], and biocompatibility and immunogenicity limitations raise great concerns. However, these observations hold only for pCNTs and, therefore, just indicate the need for further modifications in order to explore the feasibility of functionalized CNTs (f-CNTs) as safe bio-nanomaterial [5,6]. In particular, the application of f-CNTs as new nanovectors for drug delivery became doable soon after the demonstration of cellular uptake of this new material [7,8]. It is worth to mention that apart from a few cases of phagocytic incorporation inside macrophages [9,10] (which are known to be large cleaning cells able to remove foreign material including less soluble nanotubes), no uncoated pCNTs were reported to penetrate inside the cells without displaying remarkable effect. This last point should reinforce the use of f-CNTs as improved, less harmful nanovehicles, especially after our recent discovery regarding the lack of a direct correlation between the kind of functionalization on the surface of carbon nanotubes and the extent of their internalization [11-13]: either electrostatically neutral or charged f-CNTs could be taken up by cells with comparable amount, hence indicating that numerous different chemical procedures could be adapted to introduce several groups and functionalities. Further, an increased understanding of IN structural biology has opened up novel approaches to inhibit IN, such as targeting its multimerization or interaction with cellular cofactors [14]. In the paper, complex between chalcone and nanotube (6, 6) is investigated, and chalcone is used as anti-HIV drug. The chemistry of chalcones has generated intensive scientific studies throughout the world. Special interest has been focused on the synthesis and biodynamic activities of chalcones. The term 'chalcones' was given by Kostanecki and Tambor [15]. These compounds are also known as benzalacetophenone or benzylidene acetophenone. In chalcones, two aromatic rings are linked by an aliphatic three carbon chain. Chalcone bears a very good synthon, so a variety of novel heterocycles with good pharmaceutical profile can be designed. Chalcones are α- and β-unsaturated

* Correspondence: s.ghorbani.uni@gmail.com
Department of Chemistry, Islamic Azad University (Rasht Branch), Rasht, Iran

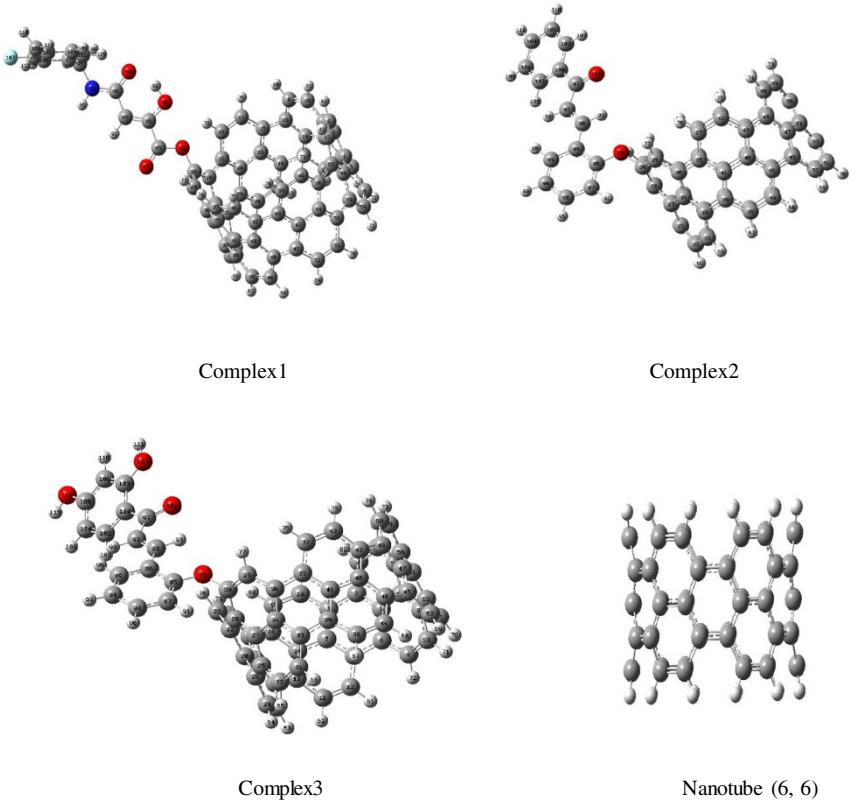

Figure 1 The optimized complex of chalcone derivative - SWCNT (6, 6) in B3LYP/6-31G(d) method at 298.15K.

ketones containing the reactive ketoethylenic group CO-CH=CH-. These are colored compounds because of the presence of the chromospheres -CO-CH=CH-, which depend in the presence of other auxochromes. Chalcones resemble the diketo acid functionality and are potential leads in designing potent IN inhibitors. Potent chalcones were identified through an NCI drug screening program [16]. The structures of chalcone are shown in Figure 2.

Results and discussion

We measured the parameters such as bond length (Å), natural bond orbital (NBO), and bond angle, dihedral angle, distances of analyzed models of the SWCNT (6, 6). The end of the nanotubes, which was saturated with hydrogen atoms, was examined by DFT at the level of B3LYP and 631G(d) standard basis set and is shown in Tables 1, 2, and 3. The electron that is given by the complexes in a reaction should make it as HOMO, while that which captured the complexes must be placed on its LUMO [17], so the atom on which the HOMO mainly scattered should be able to separate the electrons, while the atom, by holding the LUMO, should achieve electrons on this basis. HOMO-LUMO gap is usually associated with chemical stability against electronic excitation with a larger distance like greater stability [18]. The energy (kcal mol^{-1}) and dipole moments (Debye) indicate the consistency among the three complex calculations in the DFT method. The optimized configurations are shown in Figures 1 and 2. In Table 1, it becomes obvious that the complexes 2 and 3 have higher hyperconjugation energy than complex 1. The results also show that as the P increases through the sharing of hybrid atoms, the occupancy decreases. The hybrid *s* orbital shared in the oxygen atom in complex 3 is more than the hybrid *s* orbital shared in complexes 1 and 2. Most of the combined energy hyperconjugations are stable. Occupancy coefficient is smaller. Complex 2 is more stable than complexes 1 and 3. The energy hyperconjugation of complex 2 (21.25) is lesser than that of complex3. Reduced coupling energy is due to the resonance interference.

Based on the drug resonance structure, a phenolic ring is observed. In complex 2, the negative charge is located in orthoposition. However, in complex 3, the negative charge is in the oxygen group (OH). Thus,

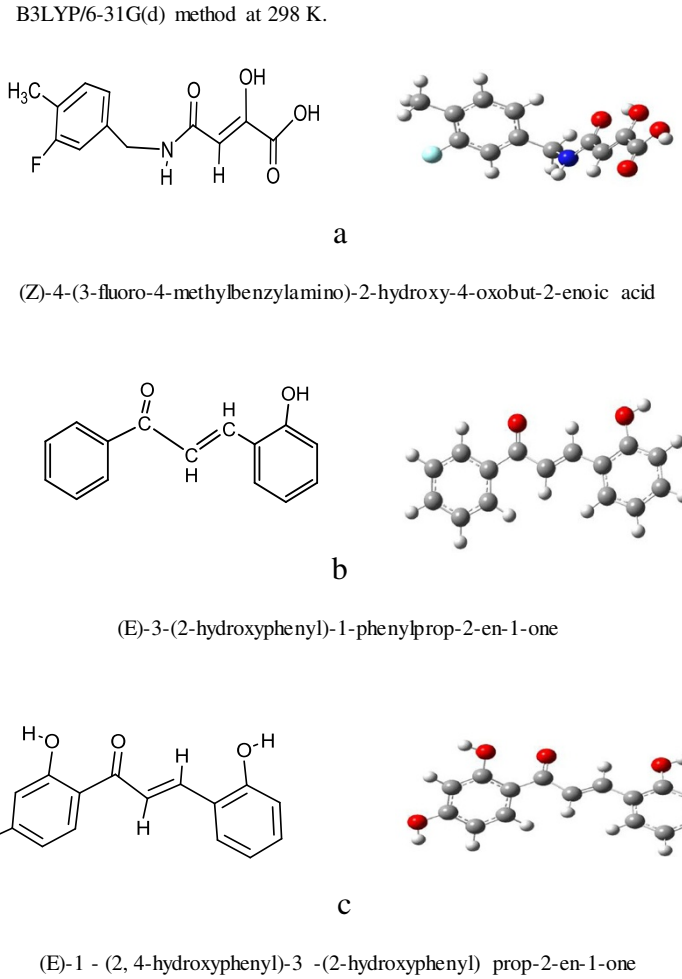

Figure 2 The structures of chalcone derivative. Optimizations were performed by B3LYP/6-31G(d) method at 298 K. **(a)** (Z)-4-(3-fluoro-4-methylbenzylamino)-2-hydroxy-4-oxobut-2-enoic acid. **(b)** (E)-3-(2-hydroxyphenyl)-1-phenylprop-2-en-1-one. **(c)** (E)-1-(2, 4-hydroxyphenyl)-3-(2-hydroxyphenyl)prop-2-en-1-one.

Table 1 The parameters of NBO complexes 1, 2, and 3 by B3LYP/631G(d) method at 298.15 K

Agent	Acceptor	Occupancy	Donor	Occupancy	Hybrid	ΣE2
Complex 1	σ* C28-30		LP(1)O84	0.03683		21.27
	π* C29-30	1.93552	LP(1)O84	0.23326	*sp*1.84	
	σ* C28-30	1.84587	LP(2)O84	0.03683	*sp*99.99	
	σ* C29-30		LP(2)O84	0.02234		
	π* C29-30		LP(2)O84	0.23326		
Complex 2	σ* C28-30		LP(1)O84	0.03694		21.25
	π* C29-30	1.93477	LP(1)O84	0.23167	*sp*1.99	
	σ* C28-30	1.84823	LP(2)O84	0.03694	*sp*12.91	
	σ* C29-30		LP(2)O84	0.02252		
	π* C29-30		LP(2)O84	0.23167		
Complex 3	σ* C28-30		LP(1)O84	0.03705		25.67
	π* C29-30	1.93368	LP(1)O84	0.24195	*sp*1.87	
	σ* C28-30	1.84353	LP(2)O84	0.03705	*sp*1.00	
	σ* C29-30		LP(2)O84	0.02139		
	π* C29-30		LP(2)O84	0.24195		

Table 2 The parameter of bond distances, bond angles, and torsional angles in B3LYP/631G(d) method optimized complexes 1, 2, and 3 at 298.15 K

Agent	Complex1	Complex 2	Complex3
$C_{30}O_{84}$	1.38360	1.38918	1.38844
$O_{84}C_{85}$	1.36355	1.37733	1.37905
$C_{85}\ldots C_{87/86}$	1.50671	1.41639	1.41556
$C_{85}=C_{86}$ or $C_{85}\ldots C_{87}$	1.34399	-	1.39631
$C_{88}\ldots N_{92}$	1.37423	-	-
$C_{88}=C_{92}$	-	1.35015	1.34867
$C_{88}=O_{93/92}$	1.22636	1.33211	-
$C_{95/92}$-C_{97}	1.51805	1.48257	1.49038
$C_{97}=O_{101}$	-	1.23025	1.22693
$C_{89/88}H_{93}$	-	1.08671	1.08697
$C_{97}C_{101/100}$	1.40144	1.50356	1.49705
$C_{102}F_{107}$	1.35539	-	-
$C_{108}O_{112}$	-	-	1.3632
$N_{92}C_{95}$	1.46093	-	-
$C_{30}O_{84}C_{85}$	119.49672	119.98567	119.72205
$O_{84}C_{85/95}\ldots C_{86}$	122.94446	115.99633	116.00968
$C_{85}\ldots C_{86}\ldots H_{89}/C_{89}$	115.63440	117.35796	117.31516
$C_{86}C_{89}=N_{92}/C_{92}$	112.89707	127.05408	126.82625
$C_{92}C_{97}=C_{101}/O_{101}$	120.54112	121.23147	121.14706
$C_{100}\ldots C_{103}F/O/H^{1}_{107}$	118.48520	117.99263	118.85317
$C_{30}O_{84}C_{85}\ldots C^{2}_{87}$	65.15798	10.06339	10.44740
$C_{85}=C_{86}C_{89}N_{92}/H^{3}_{95}$	−171.74691	178.34956	178.08447
$C_{28}\ldots C_{30}O_{84}C^{4}_{85}$	−160.04093	74.54557	75.32017
$C_{106}\ldots C_{108}O_{112}H^{5}_{113}$	-	-	179.82075
$C_{88}\ldots N_{92}C_{95}F^{6}_{107}$	179.93485	-	1.32961

complex 2 is stable. The hybrid orbital S of a compound is lower. The occupancy factor is larger. In complex 2, the hybrid and occupancy are $sp^{1.88}$ and 1.9355, respectively.

The calculations of the total energies and energy hyperconjugation (E^2) of the optimized structures, dipole moments (μ), occupancy, and hybrid orbital at B3LYP/631G(d) levels are presented in Tables 2 and 3. The DFT calculated geometric parameters for complexes 1, 2, and 3 are compared in Table 2. The bond lengths of C_{30}-O_{84} calculated for complexes 1, 2, and 3 at the DFT level are 1.383, 1.389, and 1.388 Å, respectively at the B3LYP/631G(d) level. The bond length of C_{85}...C_{87} for complex 1 is 1.50671 Å; for complexes 2 and 3, 1.41639 and 1.41556 Å, respectively. The bond length of C_{88}... N_{92} (1.37423 Å) in complex 1 is lower than the bond length of $C_{88}=C_{92}$ in complexes 2 (1.35015 Å) and 3 (1.34867 Å). This is because the electronegative nitrogen is bigger than carbon. The bond length of $C_{88}=O_{93/92}$ in complexes 1 and 2 are

Table 3 The parameter of Mulliken charge, energy HOMO/LUMO and gap energy in B3LYP/631G(d) method at 298.15 K

Agent	C_{30} Mulliken charge	Energy of HOMO (Kcal mol^{-1})	O_{84} Mulican charge	Energy of LUMO (Kcal mol^{-1})	Gap of energy
Complex 1	0.282424	−0.1579	−0.586927	−0.0889	0.06906
Complex 2	0.282510	−0.1567	−0.586736	−0.0876	0.06911
Complex 3	0.291184	−0.1538	−0.581214	−0.0855	0.06837

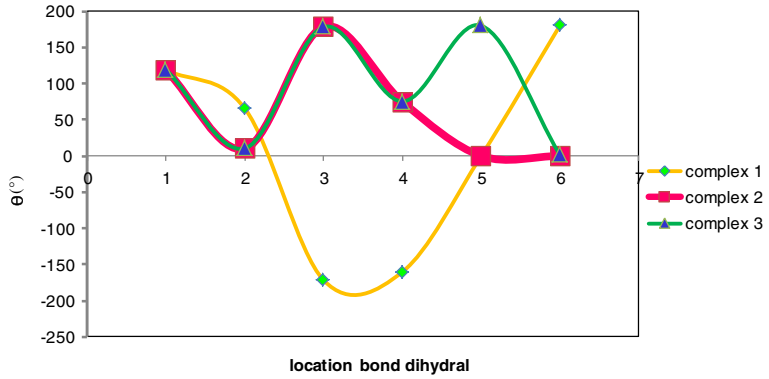

Figure 3 Parameter of dihedral angle change to locations 1, 2, 3, 4, 5, and 6 of complexes 1, 2, and 3 formed in B3LYP/631g(*d*) method at 298.15 K.

1.22636 and 1.33211 Å respectively lower than those of C=C, C...N in complexes 2, 3, and 1. The dihedral angles of $C_{100}...C_{103}F/O/H^{1}_{107}$ for complexes 1, 2, and 3 are 118.48520°, 117.99263°, and 118.85317° (in F, O, and H atoms). In locations 1, 2, 3, 4, 5, and 6, the hydra angle differences are observed in Table 1 and Figure 3. In Table 3, the Mulliken charges in donor electronegative atom O_{84} and acceptor C_{30} are negative and positive, respectively. The gap of energy of complex 2 is larger than that of complexes 1 and 3. Therefore, complex 2 is stable (Table 4).

Conclusions

Based on the above discussion, the following conclusions were made:

- The Mulliken charges of the donor atoms are negative.
- The formed bond between oxygen and carbon is stronger and has more hybrid S orbital sharing, so the bond length becomes shorter.
- There is no reaction between the nanotube and drugs in the normal body temperature.
- NBO analysis shows high hyperconjugations in all compounds.
- By increasing the hybrid *P* orbital sharing, the occupancy decreases.

Table 4 Comparison between stability energy and moment dipole of complexes 1, 2, and 3 formed in B3LYP/631g(d) method at 298.15 K

Agent	Stability energy (Kcal mol^{-1})	Dipole moment (Debye)
Complex 1	−1,900,685.711	−0.2357
Complex 2	−1,995,192.983	1.09133
Complex 3	−1,972,541.490	0.5679

Methods

A computer was used to account all calculations, which has Intel® Core™ 2 quad CPU 8400 with 4 GB RAM Gaussian 98 plan package [19] Gauss view, and nanotube model [20] maker at DFT of theory, the B3LYP useful hybrid [21] with the standard of 631G(d) basis set [22,23]. Schemes were used to display the geometric optimization of the nanotube (6, 6) with 84 atoms and compound chalcones (HIV-1 inhibitors). Separately (Figures 1, 2, and 3) then, complexes 1,2, and 3 were formed. The reaction of the nanotube and chalcone is shown in Equation 1.

$$\begin{aligned}&\text{Chalcone}\\&\quad+\text{Nanotube}(6,6)\text{Chalcone–Nanotube}(6,6)\\&\quad+H_2\end{aligned}\qquad(1)$$

Competing interests
The authors declare that they have no competing interests.

Authors' contributions
SG and MG participated in writing the manuscript. Both authors read and approved the final manuscript.

Acknowledgments
The authors would like to thank the financial support by Islamic Azad University, Rasht, Iran.

Received: 6 April 2013 Accepted: 24 May 2013
Published: 15 July 2013

References

1. Iijima, S: Helical microtubules of graphitic carbon. Nature **354**, 56 (1991)
2. Colomer, JF, Henrard, L, Lambin, P, Van Tendeloo, G: Electron diffraction study of small bundles of single-wall carbon nanotubes with unique helicity. Physic Rev B **64**, 125425 (2001)
3. Pouton, CW, Seymour, LW: Key issues in non-viral gene delivery. Adv. Drug Deliv. Rev. **46**, 187–203 (2001)
4. Singh, R, Pantarotto, D, Lacerda, L, Pastorin, G, Klumpp, C, Prato, M, Bianco, A, Kostarelos, K: Tissue biodistribution and blood clearance rates of

intravenously administered carbon nanotube radiotracers. Proc. Natl. Acad. Sci. USA **103**, 3357–3362 (2006)
5. Wong Shi Kam, N, Jessop, TC, Wender, PA, Dai, H: Nanotube molecular transporters: internalization of carbon nanotube-protein conjugates into mammalian cells. J. Am. Chem. Soc **126**, 6850–6851 (2004)
6. Pastorin, G: Crucial functionalizations of carbon nanotubes for improved drug delivery: a valuable option? Pharm. Res. **26**, 746–769 (2009)
7. Taft, BJ, Lazareck, AD, Withey, GD, Yin, A, Xu, JM, Kelley, SO: Site-specific assembly of DNA and appended cargo on arrayed carbon nanotubes. J. Am. Chem. Soc. **126**, 12750–12751 (2004)
8. Pantarotto, D, Singh, R, McCarthy, D, Erhardt, M, Briand, JP, Prato, M, Kostarelos, K, Bianco, A: Functionalized carbon nanotubes for plasmid DNA gene delivery. Angew. Chem. Int. Ed. **43**, 5242–5236 (2004)
9. Cato, MH, D'Annibale, F, Mills, DM, Cerignoli, F, Dawson, MI, Bergamaschi, E, Bottini, N, Magrini, A, Bergamaschi, A, Rosato, N, Rickert, RC, Mustelin, T, Bottini, M: Cell-type specific and cytoplasmic targeting of PEGylated carbon nanotube-based nanoassemblies. J. Nanosci. Nanotechnol. **8**, 2259–2269 (2008)
10. Gannon, CJ, Cherukuri, P: Carbon nanotube-enhanced thermal destruction of cancer cells in a noninvasive radiofrequency field. Cancer **110**, 2654–2665 (2007)
11. Cherukuri, P, Bachilo, SM, Litovsky, SH, Weisman, RB: Near-infrared fluorescence microscopy of single-walled carbon nanotubes in phagocytic cells. J. Am. Chem. Soc. **126**, 15638–15639 (2004)
12. Dumortier, H, Lacotte, S, Pastorin, G, Marega, R, Wu, W, Bonifazi, D, Briand, JP, Prato, M, Muller, S, Bianco, A: Functionalized carbon nanotubes are non-cytoxic and preserve the functionality of primary immune cells. Nano. Lett. **6**, 1522–1528 (2006)
13. Kostarelos, K, Lacerda, L, Pastorin, G, Wu, W, Wieckowski, S, Luangsivilay, J, Godefroy, S, Pantarotto, D, Briand, JP, Muller, S, Prato, M, Bianco, A: Cellular uptake of functionalized carbon nanotubes is independent of functional group and cell type. Nat. Nanotechnol. **2**, 108–113 (2007)
14. Ramkumar, K, Serrao, E, Odde, S, Neamati, N: HIV-1 integrase inhibitors: 2007–2008 update. Med. Res. Rev. **30**, 890–954 (2010)
15. Kostanecki, SV, Tambor, J: Ueber die sechs isomeren monooxybenzalacetophenone (monooxychalkone). Ber. Dtsch. Chem. Ges. **32**, 1921–1926 (1899)
16. Moyle, G, Gatell, J, Perno, CF, Ratanasuwan, W, Schechter, M, Tsoukas, C: Potential for new antiretrovirals to address unmet needs in the management of HIV-1 infection. AIDS Patient Care STDS **22**, 459–471 (2008)
17. Wrodnigg, TM, Eder, B: Topics in Current Chemistry, p. 215. Springer, Berlin (2001)
18. Stephens, PJ, Devlin, FJ, Chabalowski, CF, Frisch, MJ: Ab initio calculation of vibrational absorption and circular dichroism spectra using density functional force fields. J. Phys. Chem. **98**, 11623–11624 (1994)
19. Frisch, MJ, Trucks, GW, Schlegel, HB, Scuseria, GE, Robb, MA, Cheeseman, JR, Montgomery Jr, JA, Stratmann, RE, Burant, JC, Dapprich, S, Millam, JM, Daniels, AD, Kudin, KN, Strain, MC, Farkas, O, Tomasi, J, Barone, V, Cossi, M, Cammi, R, Mennucci, B, Pomelli, C, Adamo, C, Clifford, SO, Chterski, J, Petersson, GA, Ayala, PY, Cui, Q, Morokuma, K, Malick, DK, Rabuck, AD, et al.: Gaussian 98. Gaussian Inc., Pittsburgh, PA (1998)
20. J Crystal Soft: JCrystal. www.jcrystal.com (2013). Accessed 28 Feb 2013
21. Becke, AD: A new mixing of Hartree–Fock and local density-functional theories. J. Chem. Phys. **98**, 1372–1377 (1993)
22. Frisch, AE, Foresman, JB: Gaussian 98 User's Reference. Gaussian, Wallingford (1998)
23. Foresman, JB, Frisch, A: Exploring Chemistry with Electronic Structure Methods, 2nd edn. Gaussian, Wallingford (1996)

doi:10.1186/2193-8865-3-53
Cite this article as: Ghorbaninezhad and Ghorbaninezhad: **Simulation of nanodrug by theoretical approach.** *Journal Of Nanostructure in Chemistry* 2013 **3**:53.